JOURNAL OF SPACECRAFT AND ROCKETS
Vol. 36, No. 5, September–October 1999

Three-Stage Launch System with Scramjets

Toshiyuki Kimura* and Keisuke Sawada†
Tohoku University, Sendai 980-8579, Japan

An air-breather-based, three-stage-to-orbit reusable launch system is proposed. The first and the second reusable winged stages use turboramjet and scramjet engines, respectively. The rocket-powered third stage is expendable. The present system is designed to insert an uncrewed 2-ton payload to 300-km circular orbit inclined at 52 deg. The mission abort cases are also examined. To enhance the operational effectiveness, the landing sites for the first and the second stages are chosen to be at the same location. The calculations are made for the cases where this system is used in Japan, in the United States, and in between India and Indonesia. It is shown that the present three-stage-to-orbit launch system can exploit the potential benefit of scramjet propulsion.

Introduction

IN today's information-intensivesociety, the demand for communication satellites is ever increasing. In the past, most of these satellites have been placed in geosynchronous Earth orbit (GEO). Because a satellite in GEO needs $\frac{1}{4}$ s to send and receive the radio signal to and from the ground and because there is a limitation on available positions, a faster and less limited data transfer is required for future satellite communication. The use of the low Earth orbit (LEO) meets that requirement. Use of LEO, however, has several inherent problems. Because the altitude of the satellite is low and its speed is fast, the service area becomes narrow and changes temporally. This problem can be overcome by a system of a large number of satellites operating in a relay fashion. It is desirable that a novel launch system be developed for this new market by delivering a large number of satellites to LEO. For such a new system, reusable launch vehicles (RLV) are desirable over conventional expendable launchers because of the potentially lower launch cost of the former.

There are several competing RLV concepts. Some are rocket propulsive, and others are air-breather based. Most of the RLV concepts proposed so far envision a single-stage or a two-stage system. Because every RLV concept seems to need at least the near-term technology levels to be achieved, choosing a specific launch system solely from the technological feasibility is open to controversy. Rather, multistage launch vehicles are preferred here because of the relatively small payload assumed in the mission (to be described later) and because of the insensitivity to increases in design operating margin or payload weight when compared with a single-stage vehicle. As to the two-stage system, a fully reusable system is obviously more difficult to achieve than a partially reusable two-stage system because the former needs an orbital re-entry of the second stage. The partially reusable system, in which only the first stage is reused, is probably realizable (see, e.g., Ref. 1), but the expendable second stage tends to be large and, therefore, the system becomes costly.

In this study, we examine an alternative multistage option, namely, the air-breather-based three-stage-to-orbit (3STO) system. This 3STO vehicle is assumed to use turboramjet and supersonic-combustion-ramjet (SCR) engines for the first and the second reusable stages, respectively. The air-breathing engines are potentially highly fuel efficient. Development of a turboramjet propulsion system is almost completed.[2] However, note that choosing a 3STO system rather than a two-stage system is not obviously justified in terms of cost, unless the third stage can be significantly lighter and smaller. Our aim is to employ the SCR propulsion system for the second-stage vehicle to find a feasible scenario for possible use of the SCR engine. The 3STO configuration then enables the second stage to employ SCR engines without having to integrate a lower speed propulsion system or having to design the second stage to survive re-entry.

The 3STO system, generally, needs two landing sites for reusable two stages. The second-stage vehicle cannot takeoff by itself at the landing site because the SCR engines do not function at low speeds. Therefore, it needs to be carried back to the launch site by a carrier. These operational steps will raise the launch cost. To overcome this problem, we impose the condition that the landing sites of the first and the second stages are at the same location. This enables the second-stage vehicle to be carried back to the launch site by the first-stage vehicle. Though the first stage needs more fuel to reach the common landing site, the system will become operationally highly effective.

To evaluate the performance of such a system, the hypersonic aerodynamic characteristics are first calculated for the three vehicles involved. Sizing and weight estimation of the vehicle is then carried out using the Hypersonic Aerospace Sizing Analysis (HASA) database.[3] Flight paths for the three selected combinations of the launch and the landing sites are calculated and compared.

Description of Vehicle

Design Concept

Most planned LEO satellites have a mass of about 0.5 ton or less. Their orbit altitudes and orbital angles vary over a substantial range. Such mass and orbit requirements can be probably met by a launch vehicle capable of delivering a 2-ton payload to the orbit at an altitude of 300 km inclined at 52 deg.

As already above, the system uses the turboramjet and the SCR engines for the first and the second reusable stages, respectively, and the rocket engines for the third expendable stage. Because the first and the second stages must fly to their landing site, they must be winged vehicles. The third stage makes a ballistic flight, and so does not need wings. To avoid possible shift of the center of gravity due to the consumption of fuel or the release of the upper stages, the second stage is mounted on the first stage in piggyback. The third stage is mounted in between the dual fuselage of the second stage, although the split fuselage can cause serious aerodynamic and structural problems, which must be solved. This configuration is chosen to avoid the larger shift of the center of gravity at the first staging separation. The mated configuration is shown schematically in Fig. 1.

Geometry of Proposed Vehicle

The first stage is given a double-delta wing geometry because the shift of the aerodynamic center between the subsonic and the hypersonic speed ranges is relatively small for this geometry. Vertical stabilizers are provided at the tip of the wings. The propulsion system

Received 13 November 1997; presented as Paper 98-0303 at the AIAA 36th Aerospace Sciences Meeting, Reno, NV, 12–15 January 1998; revision received 27 February 1999; accepted for publication 27 February 1999.

*Graduate Student, Department of Aeronautics and Space Engineering; currently Research Engineer, Gifu Technical Institute, Kawasaki Heavy Industries, Kakamigahara 504-8710, Japan.

†Professor, Department of Aeronautics and Space Engineering. Senior Member AIAA.

Table 1 Geometrical parameters of the proposed 3STO

Characteristics	1st Stage	2nd Stage	3rd Stage
Length, m	50	26	16
Span, m	28	20	4
Height, m	6	7	4
Nose radius, m	0.1	0.3	0.8
Tank volume, m^3	706.5	197.4	21
Number of engines	ATR × 4	SCR × 2	RL10A × 1
Thrust, ton	120	68.7	10.1
Specific impulse, s	1800–4200	400–4000	451

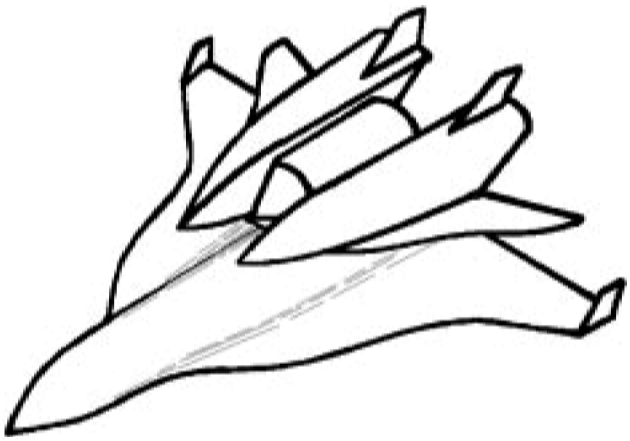

Fig. 1 Proposed 3STO concept.

consists of four air–turboramjet (ATR) engines[2] and is being developed at the Institute of Space and Astronautical Science of Japan. These engines burn liquid hydrogen and function from Mach 0 to Mach 6. We assume four engines are installed under the fuselage. Use of fuels other than liquid hydrogen may have a significant impact on the design of the first-stage vehicle; such a case is not considered because no data are available for the performance calculation.

Though the thrust of the ATR engine is only 10–15 ton in the baseline design,[2] we assume 30 ton in this study. This makes the thrust-to-weight ratio (T/W) of the present engines to be greater than 6, which is not easily attainable with present technology. We expect that such an optimistic performance can be achieved not only by the reduction of weight using advanced materials, but also by a sophistication of aerodynamic design in the integration of the propulsion system. Lighter weight could be achieved partly by exchanging components after a number of uses.

The configuration of the second stage is optimized mainly for hypersonic flight. At low subsonic speed, because of the shortage of the lift force, a para-wing[4] is deployed for approach to and landing at the landing site. Use of a para-wing may complicate the design of the second stage, but is assumed here particularly for securing the amount of lift force needed for abort landing. The second-stage vehicle has two SCR engines functioning at Mach numbers between 4 and 12 by burning liquid hydrogen. The performance data of this engine are obtained from Ref. 5.

The third stage is a conventional rocket. It uses an RL10A-4-1 engine for propulsion. This has the highest thrust among the series of RL10 rocket engines. It uses liquid hydrogen and liquid oxygen for burning.

The parameters of the present launch system are listed in Table 1. Vehicle geometries are shown in Figs. 2a–2c. The weights of these vehicles are estimated by using the HASA database. The results are presented in Table 2. Note that the present T/W value for the SCR engine is quite high, as can be calculated from Tables 1 and 2. The empirical formula for deriving the weight of SCR engine used, which is based on past examples of SCR engines, can be found in Ref. 5.

Aerodynamic Characteristics

Hypersonic aerodynamic characteristics for the present vehicle were calculated by an inviscid Newtonian method. The calculations

Table 2 Estimated weights of 3STO system

Parameter	First stage, ton	Second stage, ton	Third stage, ton	Overall, ton
Airframe	43.70	19.45	1.47	64.62
Fuselage	10.96	6.22	1.12	18.30
Wing	18.97	6.11	——	25.08
Stabilizer	0.29	0.66	——	0.95
TPS	4.48	2.74	0.35	7.57
Landing gear	9.00	2.52	——	11.52
Para-wing	——	1.20	——	1.20
Engines	17.97	6.29	0.17	24.43
Subsystem	11.56	8.11	0.73	20.40
Hydraulics	0.55	0.38	0.06	0.99
Avionics	3.26	2.30	0.42	5.98
Electronics	1.25	0.65	0.14	2.04
Equipment	6.50	4.78	0.11	11.39
Empty weight	73.23	33.85	2.37	109.45
Propellant	50.19	28.04	8.90	87.13
Payload	——	——	——	2.00
Gross weight	——	——	——	198.58

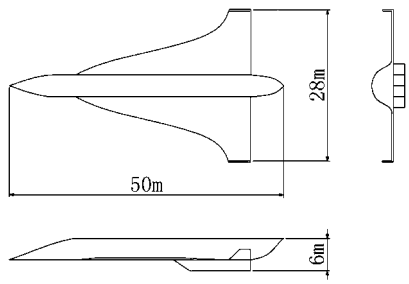

a) First stage

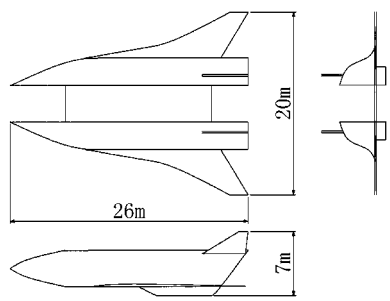

b) Second stage

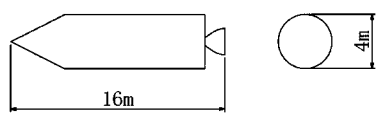

c) Third stage

Fig. 2 Vehicle geometry.

were carried out for each of the three stages, complete configuration (type I) and second plus third stages (type II). The calculated lift-to-drag ratio (L/D) in the hypersonic regime is presented in Fig. 3 as a function of angle of attack. Aerodynamic characteristics for the first-stage and second-stage vehicles in the subsonic to supersonic regime are shown in Figs. 4a and 4b, respectively, and were obtained from the formulas given in Ref. 6.

Staging Maneuvers

There is a common and severe problem inherent at staging: the recontact between the two separating vehicles. We describe the staging maneuvers of the present system next. At the first staging, the engines of the first stage are throttled, and at the same time, the air brake is opened. The second stage is mounted on the first stage using a rail, and the first stage slides backward relative to the second stage.

At the second staging, the third stage is to leave ahead of the second stage. Because the third stage is embedded inside the shock cone generated at the nose of the second stage, it is likely to be

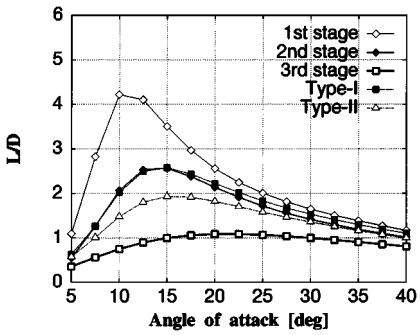

Fig. 3 Calculated L/D by inviscid Newtonian method.

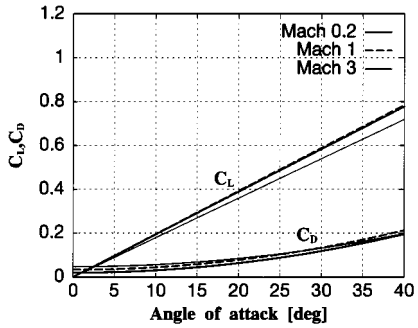

a) First-stage vehicle

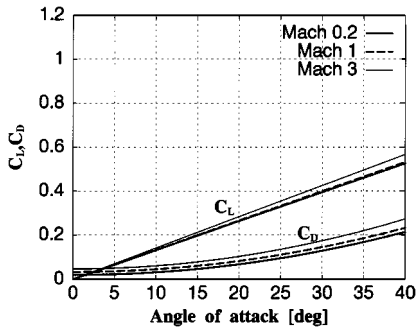

b) Second-stage vehicle

Fig. 4 Aerodynamic characteristics at Mach numbers 0.2, 1.0, and 3.0.

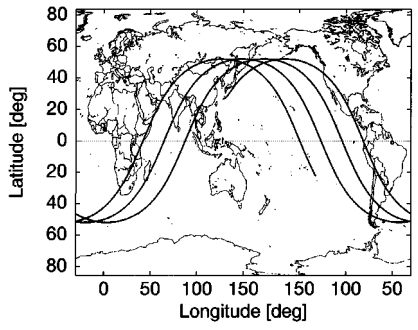

Fig. 5 Orbit inclined at 52 deg.

decelerated due to the pressure drag. Therefore, we assume a wire catapult driven by small motors to push the third stage forward during the staging. The second stage is assumed to be decelerated by the air brake.

Mission Scenarios

The orbit inclined at 52 deg covers most of the major cities in the world (see Fig. 5); thus, the satellites in this orbit can have wider service areas. Therefore, the present system is designed with the requirement that a 2-ton payload be delivered to a circular orbit at 300-km altitude inclined at 52 deg.

Table 3 Candidates for launch and landing site

Case	Launch site	Landing site
1	Okinawa	Tokachi
2	Kennedy Space Center	Maine
3	Sriharikota	Sumatra

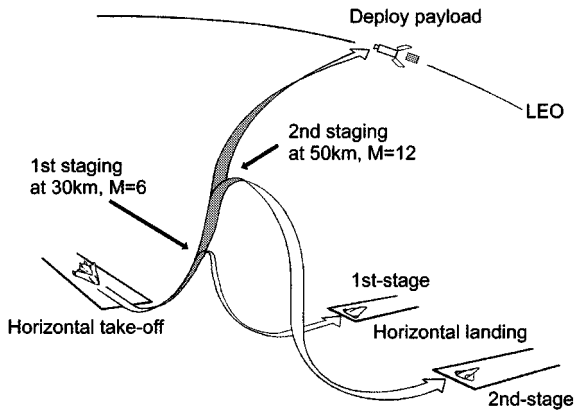

Fig. 6 Mission scenario for 3STO concept.

The mission for the 3STO system is shown in Fig. 6. The present launch vehicle takes off horizontally and ascends with ATR engines on the first stage. In this ascending phase, the vehicle flies with a constant dynamic pressure (20 kPa). The first staging is scheduled at 30 km, at Mach 5–6. Then the second stage ascends with SCR engines. The second staging is carried out at 50 km, at Mach 11–12. Finally, the third stage ascends by a rocket engine and deploys a payload to LEO. The first and the second stages fly back to the landing site after staging and land horizontally. At approach and landing, the second stage vehicle deploys a para-wing when the speed of the vehicle reduces to Mach 0.5. These two vehicles fly back to the launch site for the next mission. The first stage carries the second stage back to the launch site. The profitability of the system is greatly improved by this procedure.

The flight path of the vehicle should be chosen carefully so as not to cross any populated area. The three possible combinations of the launch and the landing sites appropriate for the present launch system are listed in Table 3. We further impose the condition that the vehicle can return back to the landing site when two ATR engines break down before the first staging.

Assuming sufficient performances of both ATR and SCR engines at the dynamic pressure of 20 kPa seems highly optimistic, though these were found to be necessary for materializing the present design. This, as well as the assumed weight of these engines, should be examined thoroughly again in a more detailed design.

Flight Path Analysis

Using the earlier obtained aerodynamic characteristics and weights of the vehicles, we now calculate the flight paths by using a three-degree-of-freedom technique. In the trajectory calculation, we do not account for trim in the pitch plane. We change three parameters, i.e., pitch, roll angle, and throttle, so as not to violate the following constraints: 1) the total acceleration of the vehicle does not exceed $3g$, where g is the acceleration of gravity, 9.8 m/s^2, and 2) the maximum wall temperature to a spherical nose of each radius listed in Table 1 is below 1600°C, which is a tolerable level for typical thermal protection system (TPS). The heating rate at the stagnation point of the nose is calculated by the formula of Ref. 7. The surface temperature at that point is obtained by imposing an equilibrium radiation condition.

Case 1

In case 1, the launch vehicle takes off from the Okinawa island. At takeoff, the calculated takeoff velocity is 152.45 m/s and the angle of attack is 20 deg after a 30-s run on a 2500-m runaway. It then ascends with a constant dynamic pressure (Fig. 7). The operational parameters are listed in Table 4. The vehicle banks to the

Table 4 Parameters of the flight for three cases

Item	Case 1	Case 2	Case 3
1st Stage			
Burn start, s	0	0	0
Burn end, s	780	780	780
1st Staging			
Time, s	780	780	780
Airspeed, m/s	1532	1532	1540
Altitude, km	30.3	30.3	30.4
2nd Stage			
Burn start, s	780	780	780
Burn end, s	1075	1075	1075
2nd Staging			
Time, s	1075	1075	1075
Airspeed, m/s	3767	3792	3781
Altitude, km	50.5	50.2	49.8
3rd Stage			
Burn start, s	1075	1075	1075
Burn end, s	1455	1454	1454
Coasting start, s	1455	1454	1454
Coasting end, s	2167	2181	2164
Orbit insertion			
Burn start, s	2167	2181	2164
Burn end, s	2184	2196	2181
1st Stage after staging			
Glide			
Start, s	780	780	780
Remaining fuel, ton	16.8	16.8	16.8
Airspeed, m/s	1532	1532	1540
Altitude, km	30.3	30.3	30.4
End, s	1250	1250	1250
Airspeed, m/s	523	427	556
Altitude, km	18.1	17.2	18.1
Cruise, 1st stage			
Burn start, s	1250	1250	1250
Burn end, s	3457	3670	3435
Airspeed, m/s	589	497	829
Altitude, km	20.2	20	22.1
Approach and landing			
1st Stage			
Start, s	3457	3670	3458
Remaining fuel, ton	0.0	1.0	0.0
Airspeed, m/s	643	582	1034
Altitude, km	22.0	22.3	25.0
End, s	3978	4167	4131
Airspeed, m/s	0	0	0
Altitude, km	0	0	0

Item	Case 1	Case 2	Case 3
2nd Stage after staging			
Glide and landing			
Start, s	1075	1075	1075
Remaining fuel, ton	0.239	0.025	0.295
Airspeed, m/s	3767	3792	3781
Altitude, km	50.52	50.24	49.80
End, s	1872	1676	2579
Airspeed, m/s	0	0	0
Altitude, km	0	0	0
Maximum acceleration			
1st Stage, *g*	1.17	1.35	1.16
Time, s	1279	939	930
Airspeed, m/s	537	1140	1215
Altitude, km	17.4	27.8	27.9
2nd Stage, *g*	1.54	2.89	1.45
Time, s	1214	1244	1075
Airspeed, m/s	3313	3088	3781
Altitude, km	41.7	38.5	49.8
3rd Stage, *g*	2.31	2.28	2.30
Time, s	2183	2196	2180
Airspeed, m/s	——	——	——
Altitude, km	300	300	300
Maximum dynamic pressure			
1st Stage, kPa	22.3	22.4	27.1
Time, s	123	124	2821
Airspeed, m/s	216	217	1031
Altitude, km	2.6	2.6	26.5
Angle of attack, deg	12.0	12.0	9.0
2nd Stage, kPa	20.4	29.2	20.4
Time, s	788	1420	789
Airspeed, m/s	1567	1803	1580
Altitude, km	30.5	30.0	30.7
Angle of attack, deg	11.1	8.6	11.0
3rd Stage, kPa	6.8	7.2	7.5
Time, s	1076	1076	1076
Airspeed, m/s	3770	3792	3785
Altitude, km	50.6	50.3	49.8
Angle of attack, deg	13.3	13.3	13.3

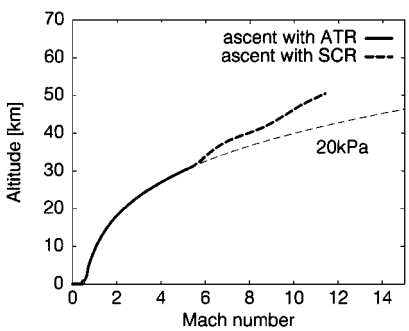

Fig. 7 Ascent flight path with air-breathing engines.

left and heads toward the target inclination angle during this phase. After 780-s from takeoff, first staging is performed. The staging conditions are: Mach 5.07, altitude 30.28 km, remaining propellant 16.8 ton, and flight-path angle 0.91 deg. Then the vehicle ascends along the trajectory shown in Fig. 7. Second staging occurs 1075 s after takeoff. The conditions are Mach 11.42, altitude 50.52 km, remaining propellant 0.24 ton, and flight-path angle 1.38 deg. After this, the third stage ascends with a rocket engine. At 1455 s, the third stage enters the coasting phase. At 2167 s, it reaches the target altitude and burns an engine to insert into the destination orbit.

The flight paths in the vertical plane are shown in Fig. 8a. After the first staging, the first-stage vehicle flies to Tokachi by cruising (Fig. 8b). The second-stage vehicle glides to Tokachi after releasing the third-stage vehicle. The acceleration histories exerted on each vehicle are shown in Fig. 8c. The wall temperatures at the nose of each stage are shown in Fig. 8d. The wall temperature of the second stage becomes the highest because of the long endurance of hypersonic flight at lower altitude. The propellant mass vs the flight Mach number along the flight path is shown in Fig. 8e for each stage.

Case 2

In case 2, the vehicle takes off from Kennedy Space Center, Florida. The ascent trajectory is almost identical to case 1. This is because the latitude of launch site and the geographical features resemble those for case 1. The second stage flies to Maine without engine burn. The first stage also cruises to Maine. The total acceleration acting on the second stage in this fly-back phase becomes the highest (Table 4) among the three cases examined. This is due to the tighter turn it has to perform to reach the landing site. The flight paths for this case are shown in Fig. 9.

Case 3

This is the case where the vehicle flies between two countries. The launch site is Sriharikota (SHAR Center), India. The vehicle

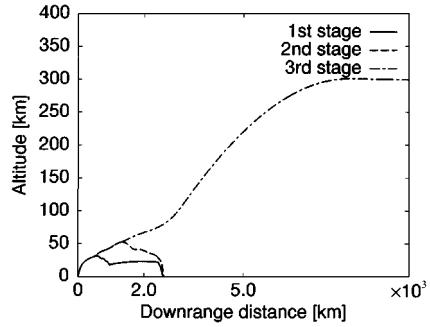

Fig. 8a Downrange map of altitude for case 1.

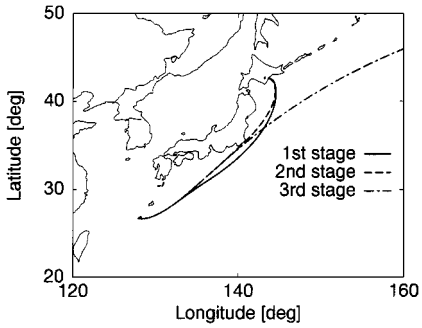

Fig. 8b Flight path for case 1.

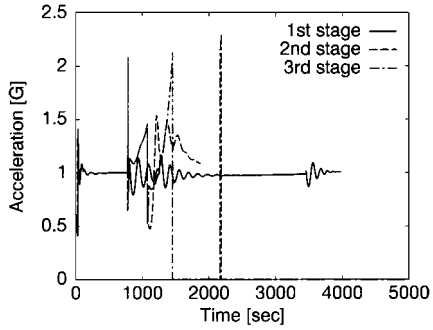

Fig. 8c Total sensed acceleration exerted on each vehicle for case 1.

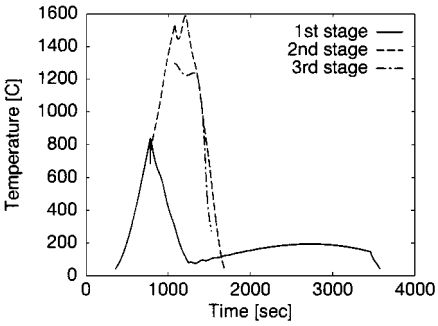

Fig. 8d Wall temperatures at nose for case 1.

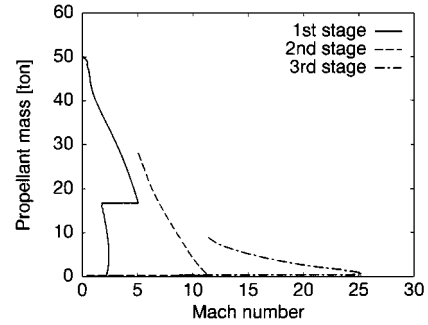

Fig. 8e Propellant mass vs flight Mach number along the flight path for case 1.

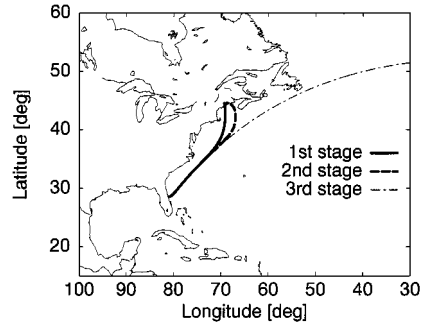

Fig. 9 Flight path for case 2.

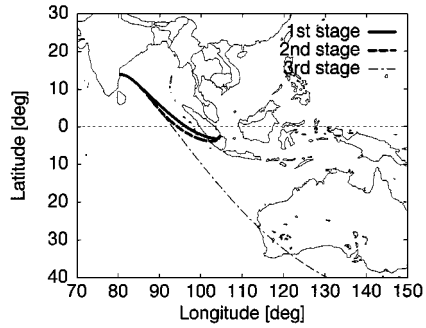

Fig. 10 Flight path for case 3.

banks to the right and flies southeast. However, the other flight status in the ascending phase is similar to the other two cases (see Table 4).

After each staging, the first and the second stages turn to the left. They are headed to and land on Sumatra, Indonesia. These flight paths are shown in Fig. 10.

Discussion

The needed components of the present 3STO system can be ready in the not so distant future. Compared with the two-stage system in Ref. 1, the weight of the expendable vehicle is significantly less. Though fuel consumption is higher than the two-stage system of Ref. 1, the overall cost is most likely lower because the cost of fuel is only a small part of the total cost and because the expendable component is smaller with the present system.

Although comparison with an all rocket propulsive system[8] can be made for various aspects, we would like to emphasize that an important advantage of an air-breathing system over rocket propulsive systems is the flexibility in performing missions that take advantage of higher specific impulse, which enables, for example, an offset launch. Furthermore, the present 3STO system has a unique self-ferry capability.

Obtained results suggest that the system is feasible in terms of flight paths and existence of a suitable set of launch and landing sites. For cases 1 and 2, the first- and the second-stage vehicles fly over the territory of one country. In case 3, however, the vehicles fly over two countries. Therefore, this plan depends on the cooperation between the two countries involved.

Let us consider the optimized plan in terms of the mission abort capability. If two engines are out before the first staging, the vehicle can return to launch site in all cases. These abort paths at Mach 4, for example, are shown in Figs. 11a–11c. The mission abort capability after the first staging, on the other hand, becomes different for each case. Assume that all of the SCR engines during the ascending phase suddenly turn out, and the abort flight is immediately initiated. For case 1, shown in Fig. 11a, the vehicle can abort the mission at Mach 10. The suitable landing site would be the Sendai airport. For Mach 7–8, the Hamamatsu airport can be chosen as the emergency landing site. However, it is impossible to abort the mission below Mach 7. For case 2, the mission abort of the second stage is possible only when the velocity is faster than Mach 10. The landing site for this case could be Boston airport (Fig. 11b). For case 3, it is also impossible to abort below Mach 10. Though the vehicle could fly to

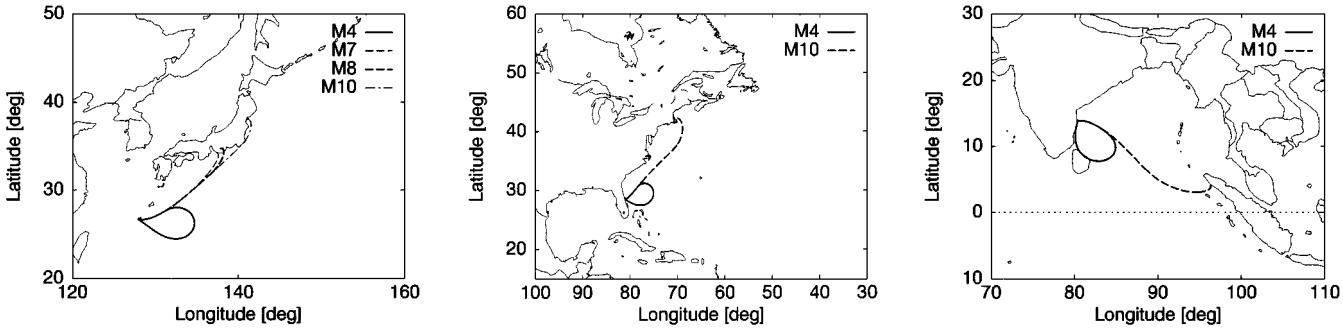

a) Case 1 **b) Case 2** **c) Case 3**

Fig. 11 Mission abort path.

Sumatra above Mach 10, there is no possible landing site there (see Fig. 11c). Note that assuming all SCR engines are shutdown during ascent is an extreme case. Unpowered abort flight may be avoided by assigning a greater number of SCR engines. A single-engine abort case is not considered in this study because the two SCR engines are positioned apart in the present design, which makes the abort flight significantly difficult.

This study shows the geographical advantage of Japan as the launch and landing site for this system. Although mission abort is impossible below Mach 10, the case of the United States is sufficiently competitive.

Conclusions

An air-breather-based 3STO reusable launch system has been proposed. By dividing the system into three stages, it can use SCR engines, effectively. Three sets of suitable launch and landing sites are selected, and the corresponding flight paths are shown for the three areas. In all cases, the first and the second stages are able to land on the same site. For the mission abort capability, differences exist among them. However, the flight path analysis indicates the feasibility of this system in all three cases.

Acknowledgments

The authors gratefully acknowledge C. Park, formerly professor at Tohoku University, and K. Mizobata for helpful suggestions.

References

[1]Takahashi, S., Mizobata, K., and Sawada, K., "Conceptual Study of a Two-Stage, Air-Breathing Reusable Launch Vehicle," *Journal of Spacecraft and Rockets*, Vol. 34, No. 5, 1997, pp. 628–635; also AIAA Paper 97-0192, Jan. 1997.

[2]Tanatsugu, N., Naruo, Y., Sato, T., Rokutanda, I., Mizutani, T., and Kashiwagi, T., "Development Study on Expander Cycle Air Turbo-Ramjet Engine," *Proceedings of the Annual Meeting and the Third Symposium on Ram/Scramjets*, Northern Section of the Japan Society for Aeronautical and Space Sciences, Sendai, Japan, 1993, pp. 211–216 (in Japanese).

[3]Harloff, G. J., and Berkowitz, B. M., "HASA-Hypersonic Aerospace Sizing Analysis for the Preliminary Design of Aerospace Vehicles," NASA CR-182226, Nov. 1988.

[4]Park, C., Menees, G. P., Bowles, J. V., Lawrence, S. L., and Davies, C. B., "Conceptual Study of a Bent-Biconic Single-Stage-To-Orbit Vehicle," AIAA Paper 95-0716, Jan. 1995.

[5]Masuya, G., and Wakamatsu, Y., "Calculation of Scramjet Performance," National Aerospace Lab., TR-987, Tokyo, Japan, July 1988 (in Japanese).

[6]Raymer, D. P., *Aircraft Design: A Conceptual Approach*, AIAA, Washington, DC, 1992, pp. 257–312.

[7]Detra, R. W., Kemp, N. H., and Riddell, F. R., "Addendum to 'Heat Transfer to Satellite Vehicles Re-Entering the Atmosphere,'" *Jet Propulsion*, Vol. 27, Dec. 1957, pp. 1256–1257.

[8]Nakajima, M., Mizobata, K., and Sawada, K., "Conceptual Design of LE-7-Based Reusable Launch Systems," AIAA Paper 98-0304, Jan. 1998.

J. A. Martin
Associate Editor